Desalination and Water Treatment
www.deswater.com

doi: 10.5004/dwt.2017.21270

91 (2017) 74–81
October

Effect of aeration rate on the performance of a novel nonwoven flat plate bioreactor

S.A. García-González*, A. Durán-Moreno

Facultad de Química, Departamento de Ingeniería Química, Universidad Nacional Autónoma de México, Distrito Federal, CP 04510, México, Tel. +52 5556225293/Fax: +52 5556225303, emails: cheko29@hotmail.com (S.A. García-González), alfdur@unam.mx (A. Durán-Moreno)

Received 20 December 2016; Accepted 29 July 2017

ABSTRACT

The aim of this work was to evaluate the effect of aeration rate (U_g) on the performance of a novel nonwoven flat plate bioreactor. Increase in U_g, ranging from 0.080 to 0.129 m/s, resulted in the increase of the apparent substrate consumption rate (8.38–11.86 mg/L h) and decrease in mixing time (from 13 to 7 min), thereby positively affecting the oxygen (kLa) and external (k_c) mass transfer. Biofilm detachment was less than 1% despite the fact that shear stress value was 1.12 Pa at the highest airflow rate. The system could treat a superficial organic loading from 13.54 up to 50 g phenol/m^2 d with almost 100% phenol removal.

Keywords: Biofilm detachment, flat plate bioreactor, nonwoven fibrous support

1. Introduction

Currently, the international trend on designing municipal and industrial wastewater treatment technology involves the construction of compact and low energy-consuming systems [1]. According to scientific research, biofilm systems have the advantages of compactness and low energy consumption over other approaches [2,3]. However, biofilm systems also have disadvantages, such as operational problems due to slow mass transfer of contaminants and nutrients to it. Moreover, when biofilm reactors have treated high organic loadings, they have presented a limitation in oxygen transfer.

Najafpour [4] reported that increasing air flow allows for the improvement of the oxygen transfer coefficient (k_La). Furthermore, González-Brambila and López-Isunza [3] demonstrated that in a biofilm system (permeable membrane), when the superficial liquid velocity was increased, the external mass transfer was reduced and the diffusion into the biofilm was improved. Nevertheless, these researchers determined that at a superficial velocity above 0.0107 m/s, the biofilm was detached from the support due to shear stress. Moreover, Arrojo [5] demonstrated that increase in the upflow velocity of the air, which involves shear stress, decreases the specific activity of Anammox granules by approximately 85%. In recent works, a complete retention of the biological material within the system is an important requirement for a successful continuous operation of immobilized bioreactors, as the submerged membrane promotes the catalytic process [6].

One of the most active research areas regarding biofilm aerobic biological systems is the analysis of the biomass supported on nonwoven materials [7]. These materials are porous fabrics and they are composed of a random array of polymeric fibers or filaments in a tridimensional structure in several layers. More frequently used polymers for biofilm systems are polyester (poly(ethylene terephthalate)), polypropylene, polyethylene and nylon [8]. In addition, these polymeric fibers can be used in several arrays allowing for the design of novel bioreactors, sponge cubes being one of the most preferred immobilization systems [9,10]. However,

* Corresponding author.

Presented at the 13th IWA Specialized Conference on Small Water and Wastewater Systems & 5th IWA Specialized Conference on Resources-Oriented Sanitation, 14–16 September, 2016, Athens, Greece.

other unexplored configurations such as zig-zag flow paths can be considered. The principal advantages of these materials are that they provide a high specific surface area for cell attachment, high and constant surface-to-volume ratio, high mechanical strength, high permeability, low cost and lower mass transfer resistance compared with microcarrier particles [11].

The novel details of the present fixed biofilm bioreactor are a horizontal zig-zag air-water flow through it, a relatively reduced air flow cross-section, microorganisms attached to a nonwoven fibrous support and a relatively high separation between fiber dishes. As a result of these design improvements, aeration rate, liquid agitation, contaminant removal rate and mass transfer coefficients were increased. Thus, the effects of aeration rate (U_g) on hydrodynamics, mass transfer and biological degradation were evaluated to obtain the necessary data to describe the operation of this type of bioreactor.

2. Materials and methods

2.1. Experimental setup

The nonwoven flat plate bioreactor consisted of an acrylic column (8.2 L, 65 cm height and 15 cm internal diameter) with eight synthetic fiber-scouring pads as support matrix (15 cm × 0.5 cm thickness, Light Duty Scrubbing Pad 9030-Scotch Brite™, 3M Company, Mexico City). Each tray was separated at a 5 cm distance, kept in form by a 14.5 cm outer diameter poly(vinyl chloride) ring and with an alternated 30% empty space intentionally left between each one to induce a zig-zag flow pattern in the vessel (Fig. 1).

The fiber-specific surface area (0.20 m^2/g) was measured by nitrogen physical adsorption (Brunauer–Emmett–Teller isotherm), and the apparent porosity (94.3%) was determined according to Hutten and Russell [8,12]. A peristaltic pump (Ismatec™ Ecoline CP 78022-40) was used to supply a constant wastewater flow through the multi-tray bioreactor. A micropore diffuser provided the free-oil airflow in the bottom. The bioreactor was operated at constant temperature (21°C ± 0.1°C) and pH was kept at 7.4 ± 0.1.

2.2. Bubble diameter

Bubble diameter was regulated by a 20 μm porous diffuser. The photos have been taken using a Sony Cyber-shot camera (DSC-W120 couples a seven megapixel sensor to a Zeiss-branded 4× optical zoom and a 2.5-inch 115,000 pixel LCD display), the image analysis in ImageJ was used to characterize the bubble size and shapes in the homogeneous flow regime in the bioreactor [13].

2.3. Inoculation and quantification of the physicochemical parameters

For inoculation, mixed liquor samples were collected from an activated sludge wastewater treatment plant at the Universidad Nacional Autónoma de México campus. Sludge samples were grown in gradually enriched phenol media, using the methodology of Mamma et al. and El-Naas et al. [14,15] until a concentration of 0.8 g/L was reached. Finally, the bioreactor was inoculated with 8.7 L of phenol-degrading adapted microorganisms, considering a biomass concentration of 1,450 mg VSS/L. Tests of the total suspended solids (TSS) and the volatile suspended solids (VSS) were performed according to the Standard Methods Guidelines [16]. The phenol concentration was evaluated by UV spectrophotometry at 270 nm according to the methodology of Mkandawire et al. [17], and pH and turbidity were measured using an Orion™ 2-Star Benchtop pH meter (Thermo Orion, USA) and a HI 98703 turbidity meter (HANNA Instruments,

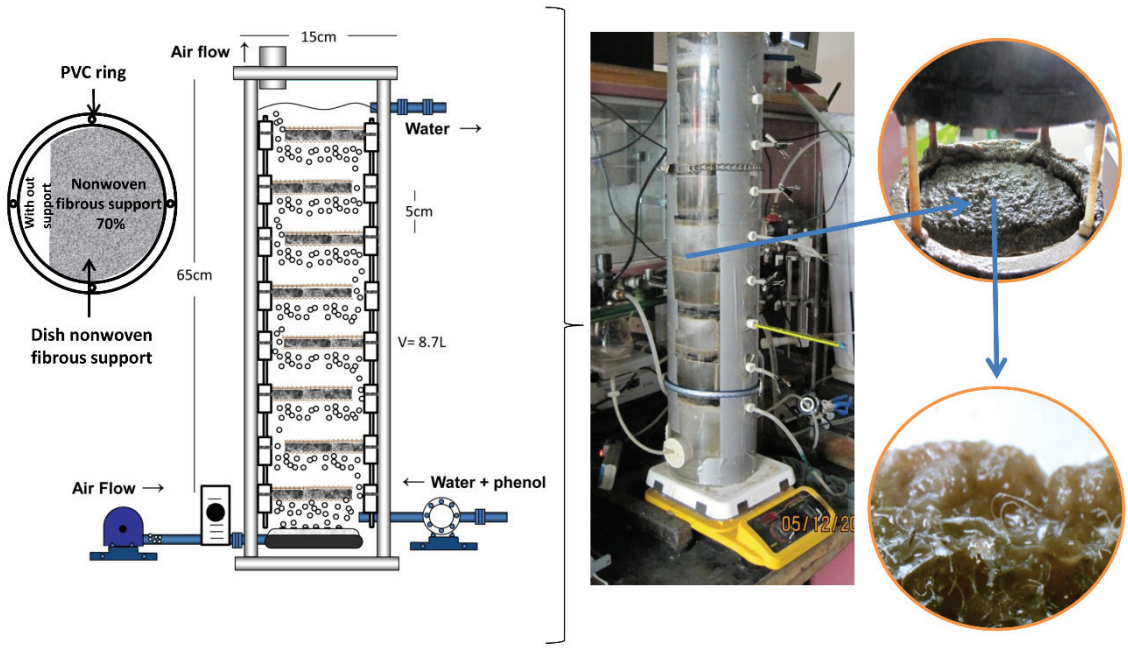

Fig. 1. Schematic diagram of the nonwoven flat plate bioreactor.

Mexico City), respectively. Biofilm cell growth was evaluated through the Monod model [1,18], which allowed the kinetic constants to be determined.

2.4. Hydrodynamics

Flow regime inside the bioreactor was measured by methylene blue dye pulse injection [19]. Concentration was measured each minute by spectrophotometry at 665 nm (Varian's Cary™ 50) until the dye's complete disappearance in it. The theoretical hydraulic residence time (HRT) used for this experiment was 2.4 h. Residence time distribution (RTD) and flow type were calculated using the dye concentration values in the biological bioreactor. Mixing times (θ) were evaluated at three different U_g values (0.064, 0.080 and 0.096 m/s). Mixing time is a key parameter used for analyzing the performance and the hydrodynamics of a bubble column, it is an important parameter used frequently to represent mixing in bioreactors [20]. Typically, all the energy input into a pneumatically agitated bubble column comes from compressed gas. The gas imparts energy to the liquid as it expands isothermally from the hydrostatic pressure at the bottom of the container to the pressure in the head zone [21]. A second source of power is the kinetic energy of the gas jet at the point of entry to the vessel, the pneumatically agitated bubble columns have a direct relation between the mixing time (θ) and the aeration rate (U_g).

2.5. Mass transfer (G/L)

Oxygen transfer from bulk gas (*G*) into the bioreactor bulk liquid (*L*) was determined by the dynamic method [22,23]. Additionally, once the biofilm was formed after a 3-week operation period, the volumetric oxygen mass transfer coefficients (k_La) were calculated by Eq. (1):

$$\frac{dC}{dt} = k_La\left(C^* - C_L\right) - \mathrm{OUR} \tag{1}$$

where dC/dt is the oxygen accumulation rate, C_L is the dissolved oxygen concentration in the bulk liquid, C^* is the oxygen saturation concentration in the bulk liquid and OUR is the oxygen uptake rate. C_L in the liquid phase was measured using a HANNA HI 9143 dissolved oxygen electrode. In the experiments, the aerator was stopped, the agitation of the system was turned on at a speed of 350 rpm, and the dissolved oxygen was subsequently measured until it decreased its value to 2.5 mg/L. Later, the agitation system was stopped, and then the aeration system started. During the aeration time, the dissolved oxygen was measured every 3 s and the values of k_La were calculated at different U_g values: 0.009, 0.021, 0.050, 0.064, 0.080, 0.096, 0.112 and 0.129 m/s.

2.6. Biofilm detachment

The biofilm detachment caused by shear stress is an instantaneous process in comparison with the biofilm growth time; the hydrodynamic (shear stress) characteristic times in a biofilm system are much smaller, by six orders of magnitude, than the characteristic times for biomass growth [24]. Shear stress was calculated using Eq. (2) [25], considering three different U_g values (0.080, 0.096 and 0.112 m/s). For each shear stress value, the biofilm detachment was evaluated by TSS in the bulk liquid.

$$\gamma = \left(\frac{\rho_L g U_g}{\mu_L}\right)^{0.5} \tag{2}$$

2.7. Mass transfer (L/S) and diffusion in the biofilm

The external mass transfer coefficient (k_c) between the outer bulk liquid (*L*) and the bulk solid (*S*) was calculated after 4 weeks of continuous operation. Then, the system was operated in batch considering four different U_g values (0.080, 0.096, 0.112 and 0.129 m/s) with 100 mg phenol/L as a model contaminant to evaluate the air flow effect in the k_c values. Additionally, the apparent substrate consumption rates at different air flows were calculated. Based on this information, k_c was calculated using the Aquasim model [26–28].

2.8. Continuous operation

The bioreactor was operated for 2 months at different superficial organic loadings of phenol, ranging from 13 to 100 g/m² d. The amounts of dissolved oxygen and phenol removal were measured to evaluate its operation.

2.9. Repeatability

Each measurement was repeated at least three times, reported values are means of the repeat measurements, error bars were added corresponding to the mean ± standard deviation.

3. Results and discussion

3.1. Acclimatization of microorganisms to phenol

In the first 50 d of the trial, a quick adaptation of microorganisms to phenol was observed, as confirmed by a close to 100% pollutant removal efficiency. After this acclimation period, the phenol-adapted biomass was used to perform different batch experiments to calculate the kinetic coefficients. The results obtained from the Aquasim model for the half-saturation coefficient (K_S) 15.47 mg/L, and the maximum growth rate (μ_{max}) 0.1158 h^{-1} were consistent with values reported in the literature [29].

3.2. Bubble diameter

Bubble diameter was regulated by a 20 μm porous diffuser; the bubbles were not in contact with the biofilm because it was inside the material of the mesh and the nonwoven protected the cell. The detachment of biological material was only on the surface of the mesh and it was less than 1% of the total microorganisms of the biofilm. This was evaluated by TSS. The average bubble size in a column has been found to be affected by gas velocity, liquid properties, gas distribution, operating pressure and column diameter [30]. Thus, the size and rise velocity of a bubble depend on each other and are

affected by the same parameters. Bubble size is affected by organic substances according to Besagni et al. [13] and the organic substances ("positive surfactants") are attracted to the bubble interface where they adsorb positively, causing a decrease of the surface tension and inducing coalescence suppression. Phenol affected the surface tension of the liquid and this created a small spherical bubble; the image analysis in ImageJ was used to characterize the bubble size distributions and shapes in the homogeneous flow regime in the bioreactor. The average diameter was 0.9137 ± 0.21 mm of 278 data. Fig. 2 shows the measured bubble size of one sample in the system.

3.3. Hydrodynamics

HRT was measured to determine the system hydrodynamics. The results are shown in Figs. 3(a) and (b). In the absence of airflow, the bioreactor behavior followed that of the plug flow

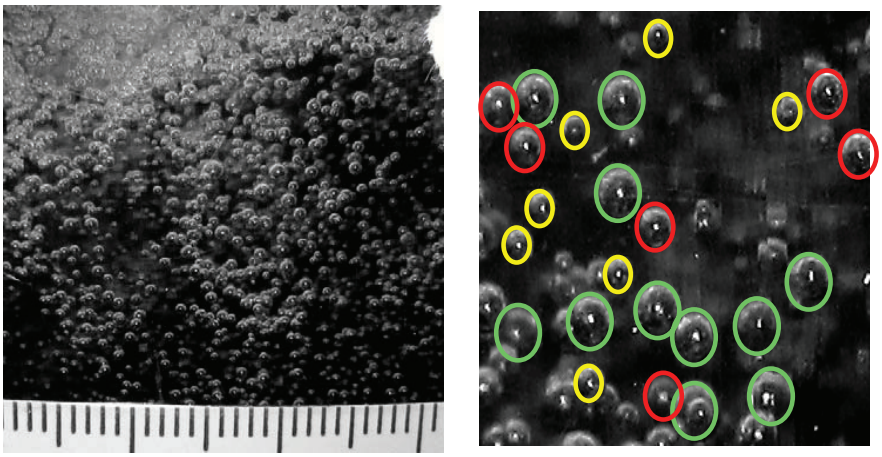

Fig. 2. Bubble size distributions and shapes in the homogeneous flow regime in the bioreactor.

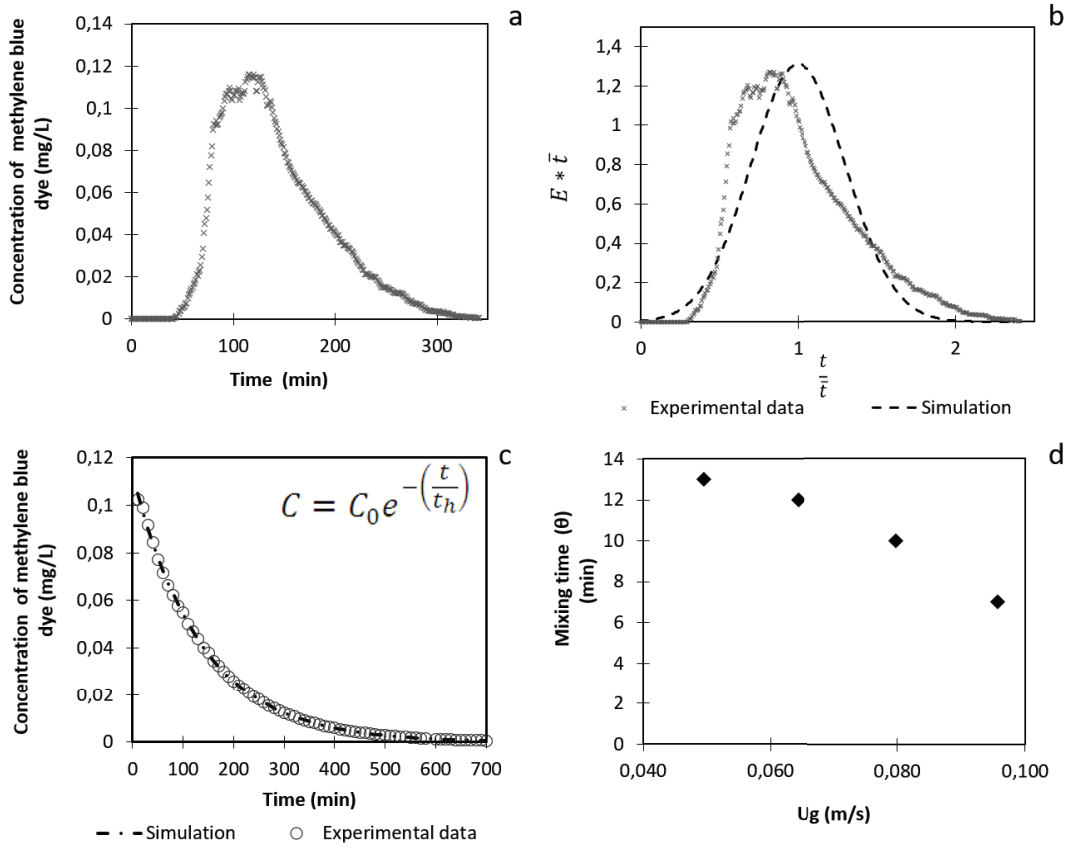

Fig. 3. (a) Determination of the RTD curve without airflow, (b) modeling the RTD curve without airflow, (c) determination of the RTD curve with airflow, (d) measurement of the mixing time (θ) in the bioreactor at different aeration rate (U_g) values.

reactor model. HRT was 142 min, which was slightly inferior to the theoretical residence time (144 min). The experimental RTD data were fitted to the normalized exit age distribution (*E*), which was calculated using a dispersion coefficient (D/uL) value of 0.0463 [19] (Fig. 2(b)). The RTD experimental curve is out of phase when superimposed to *E* due to the stagnant zones in the system. A value of 9.2% was obtained for these zones using the method of Pérez and Torres [31].

With an aeration rate (U_g), value of 0.064 m/s in the system, the bioreactor behaved as a completely mixed flow; this trend was obtained from the comparison of these results with the continuous stirred-tank reactor (CSTR) mathematical model. Based on origin software simulation, a correlation coefficient of 0.99936 was found between the experimental data and the CSTR model, as shown in Fig. 3(c).

3.4. Mixing time

A few minutes after the injection, a complete mixing system was achieved, with the resulting concentrations of methylene blue dye shown in Fig. 3(c). The point when the system reaches the complete mixture is known as mixing time (θ), which indicates the degree of agitation in the liquid. The experiments were conducted at various air flows, increasing the aeration rate from 0.050 to 0.096 m/s, while θ was reduced from 13 to 7 min, as shown in Fig. 2(d).

3.5. Mass transfer (G/L)

Fig. 4(a) shows the experimental data of dissolved oxygen at different U_g values in the bioreactor. When U_g values are increased above 0.096 m/s, dissolved oxygen curves were found to be very similar. The calculated coefficients k_La are shown in Fig. 4(b), where increasing U_g was also found to increase k_La . However, when U_g value was higher than 0.096 m/s, it did not have a significant effect over k_La, which varied only from 1.02 to 1.10 min^{-1}. It can be established that an increase in the air flow above the previously mentioned value does not promote oxygen transfer into the system. At different U_g values, from 0.009 to 0.129 m/s, k_La value increased from 0.12 to 1.10 min^{-1}; this demonstrates that k_La is function of U_g.

When the condition of oxygen saturation was obtained, the aeration system was stopped to determine OUR value in the bioreactor. The oxygen concentration in it decreased linearly after 50 min, resulting in an OUR value of 0.0179 mg_{O_2}/Lmin, demonstrating that the biomass in the biofilm was constant.

3.6. Biofilm detachment

When the bioreactor operated in batch mode, the detached solids in it were measured as TSS at different shear rate values (0.88, 0.97 and 1.05 Pa). The VSS in the bioreactor never exceeded 20 mg/L (Fig. 5(a)), so all the biomass can be considered to be attached to the nonwoven fibrous support, and a minimal fraction was suspended in the bioreactor. The detached solids were less than 1% of the total biofilm in the support despite the shear stress value of 1.12 Pa at the highest air flow rate; this is important because the support could immobilize a large amount of active microorganisms

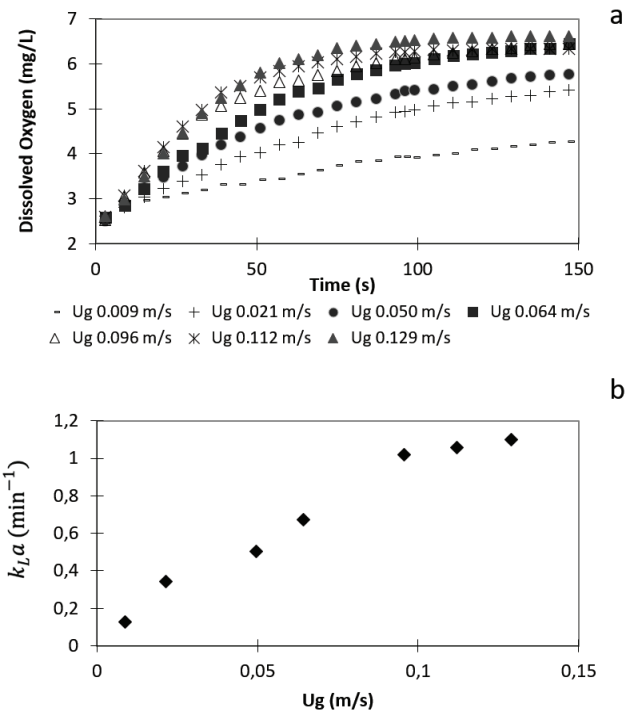

Fig. 4. (a) Dissolved oxygen measurements at different aeration rate (U_g) values, (b) values of the volumetric oxygen mass transfer coefficients (k_{La}) considering different aeration rate (U_g) values.

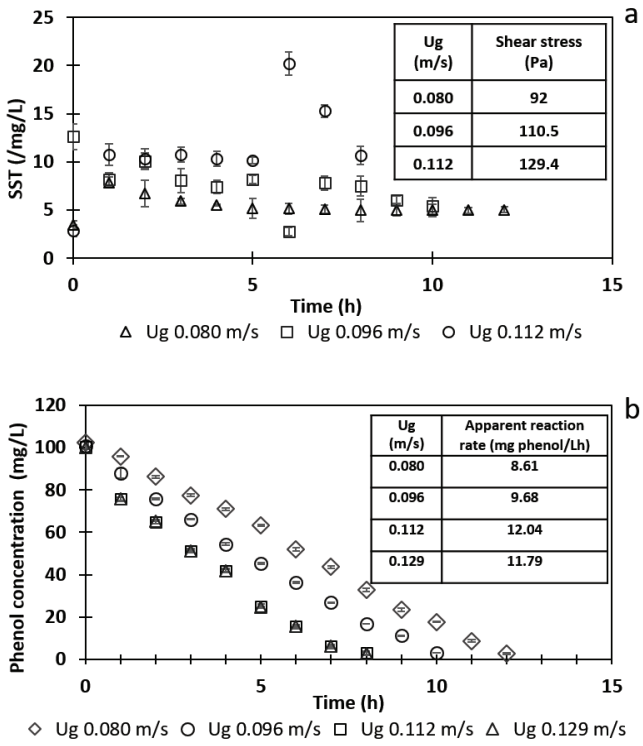

Fig. 5. (a) Biofilm detachment in the bioreactor at different aeration rate (U_g) values, (b) apparent reaction rate at different aeration rate (U_g) values.

(1.44 g VS/$g_{support}$) to degrade the phenol. The total active biomass in the nonwoven fibrous support was 61.3% according to the catalase activity test [32].

The nonwoven fibrous support immobilized the biofilm in a fashion similar to traditional supports; in addition, it protected the cells of shear stress from the aeration rates.

3.7. Operation in the batch bioreactor to evaluate the mass transfer L/S

Several experiments were performed at different airflow conditions in the bioreactor. Fig. 5(b) shows phenol concentration at different U_g values, ranging from 0.080 to 0.129 m/s. In all these experiments, the initial phenol concentrations were 100 mg/L and the concentrations were measured until the disappearance of the phenol. Fig. 5(b) shows that reaction time decreased from 12.1 to 8.34 h when the U_g values increased. González-Brambila and López-Isunza [3] demonstrated that if the Reynolds number increases, then the boundary layer thickness decreases. Therefore, the reaction rates increase mainly due to increase of k_c. Recalling that k_c = D/LL, in this case, D is the diffusion coefficient of phenol in water and LL is the boundary layer thickness; as a result of the decrease in the thickness, the mass transfer and the reaction rate also increased. The reaction rate increased 50% (from 8.37 to 11.79 mg_{phenol}/L h) when the bioreactor was operated at the highest aeration rate (0.1290 m/s). Note that the measurements of dissolved oxygen were similar and always greater than 7.4 mg/L, indicating that reactions were not limited by the concentration of dissolved oxygen in all the experiments.

3.8. Mass transfer (L/S), modeling of the batch bioreactor using the Aquasim model

To model the system using the Aquasim model, it was considered that (1) the values of K_s and μ_{max} were obtained in a suspension system; (2) the hydrodynamics of the container was considered as a biofilm system with *L* completely mixed; (3) the diffusion coefficient of contaminant in the biofilm ($D_{biofilm}$) was estimated from the degradation profiles that indicated phenol concentration in Fig. 5(b) when the bioreactor was operated in batch mode. With the U_g value of 0.1290 m/s, the system did not register any significant change in reaction rate in comparison with the system with the U_g value of 0.112 m/s. Then, it was assumed that the boundary layer thickness was at least 0.1 μm. The value of the $D_{biofilm}$ was 2.36 × 10^{-8} m^2/h, which was used to simulate other degradation profiles with an external mass transfer opposed to the transport of the contaminants.

The simulation was performed based on the Aquasim model using two different kinetic types: Monod and zero order. As shown in Fig. 6(a), the Monod kinetic does not appropriately represent the experimental data: the mean relative deviation was 82%, which was calculated according to the method of Kablan et al. [33]. As a result, the diminution of phenol concentration at the time was similar to a straight line, which was simulated using a zero-order kinetic, as shown in Fig. 6(b), where mean relative deviation was 6.2%; thus, the second simulation is more representative for the experimental data. Finally, external mass transfer coefficients (k_c) changed from 3.67E^{-05} to 2.68E^{-04} m/s.

3.9. Continuous operation biofilm bioreactor

The biofilm type system can treat high superficial organic loading of contaminants in continuous operation. In this experimental stage, organic loadings of phenol (from 13 to 100 g/m^2 d) were tested, and the system behavior was stable. Fig. 7 presents contaminant removal and dissolved oxygen concentration during the experiments. The removal of the contaminant was greater than 99%, and bioreactor behavior was stable, with a superficial organic loading of phenol smaller than 50 g/m^2 d. However, at higher organic loadings (from 50 to 100 g/m^2 d), there was an oxygen deficit in the apparatus. This was present in the bulk liquid in the continuous operation; in this experimental stage, aeration rate was maintained constant and value was 0.112 m/s. On the other hand, in the batch tests, the effect of aeration rate was tested

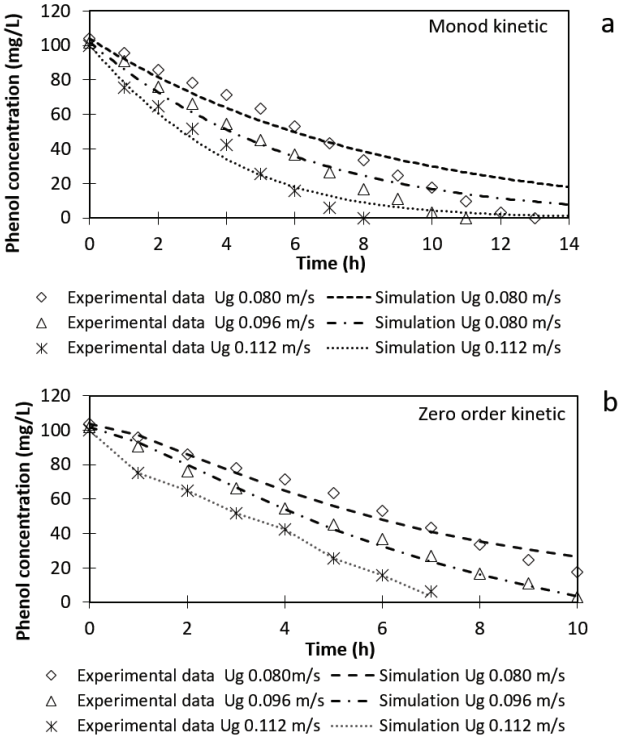

Fig. 6. (a) Modeling at different aeration rate (U_g) values with the Monod kinetic, (b) modeling at different aeration rate (U_g) values with the zero-order kinetic.

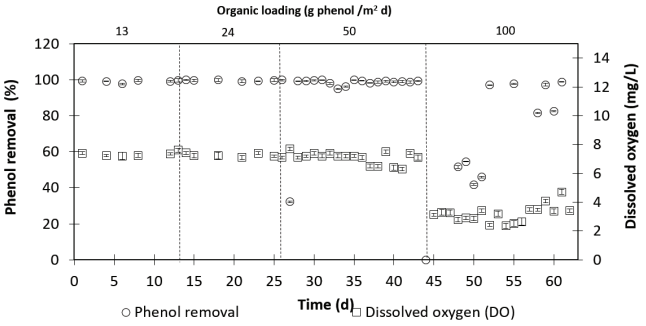

Fig. 7. Dissolved oxygen and phenol removal in a continuous bioreactor.

Table 1
Comparison of biofilm technology

Biofilm process		COS (g DBO/m^2 d)	COV (kg DBO/m^3 d)	Removal %
MBBR[a]	High rate	>20	–	75–80
	Normal rate	5–15	–	80–90
	Low rate	5	–	98
BAF[a]			1.5–6	90–65
Rotating biological contactors		15–30	–	65–90
Trickling filter[a]		20–39	0.32–0.96	50–75
Nonwoven flat plate bioreactor[b]		32.54–263.0	14.31–100.8	86.8–99.9

[a]Water Environment Federation [1].
[b]This work.

in the bioreactor, aeration rate improved oxygen mass transfer agitation and reaction velocity. In both experiments, the organic loading was the parameter that had more influence in oxygen deficit.

Finally, a comparison of existing technologies for the treatment of wastewater was carried out. Table 1 shows the organic loadings in which these systems are conventionally operated; it also shows the elimination efficiencies of the system.

4. Conclusions

The innovative multi-tray bioreactor studied improves some problems detected in conventional biofilm wastewater reactors. Hydrodynamics, kinetics and mass transfer (G/L, L/S) were evaluated in a novel nonwoven flat plate bioreactor. Gas velocity in it had influence on mixing time. Air flow values above 0.096 m/s of U_g did not exert a significant effect on k_La. Gas velocity did not increase the detachment on the nonwoven fibrous support. The amount of solids detachment was less than 1% of the total biofilm, and the support immobilized microorganisms to degrade phenol (1.44 g biomass/g support), where 61.3% were active. When the aeration rate increased (0.080–0.129 m/s), the apparent reaction rate increased by 50% and, as a consequence, k_c values increased. Mass transfer (G/L) and (L/S) were evaluated and modeled in the bioreactor, which presents a stable operation at a superficial organic loading of phenol of 50 g/m^2 d. It is recommended to continue the study of these types of reactors to determine whether it is possible to carry out the scale of the technology.

Abbreviations

G — Bulk gas
L — Bulk liquid
S — Bulk solid
WEF — Water Environment Federation

Variables

C_L — Dissolved oxygen concentration in the bulk liquid, mg_{O_2}/L
C^* — Oxygen saturation concentration in the bulk liquid, mg_{O_2}/L
d_p — Bubble diameter, mm
D — Diffusion coefficient of phenol in water, m^2/s
$D_{biofilm}$ — Diffusion coefficient of phenol in the biofilm, m^2/h
dC/dt — Oxygen accumulation rate, mg_{O_2}/L_s
D/uL — Dispersion coefficient
E — Normalized exit age distribution
HRT — Hydraulic residence time, min
g — Gravitational acceleration, m/s^2
k_c — External mass transfer coefficient, m/s
k_La — Volumetric oxygen mass transfer coefficient, min^{-1}
K_s — Half-saturation coefficient, mg/L
LL — Boundary layer thickness, μm
OUR — Oxygen uptake rate, mg_{O2}/L min
RTD — Residence time distribution, s^{-1}
TSS — Total suspended solids, mg/L
U_g — Aeration rate, m/s
VS — Volatile solids, g
VSS — Volatile suspended solids, mg/L

Greek

γ — Shear stress, Pa
θ — Mixing time, min
μ_s — Kinematic viscosity, m^2/s
μ_{max} — Maximum growth rate, h^{-1}
μ_L — Liquid viscosity, pa s
ρ_L — Liquid density, kg/m^3

Acknowledgments

The authors acknowledge the financial support for this research from the Dirección General de Asuntos del Personal Académico (DGAPA, PAPIIT-IT/102415) of the Universidad Nacional Autonóma de México (UNAM), and the Consejo Nacional de Ciencia y Tecnología (CONACYT México) for the PhD scholarship to S.A.G.G. as well as Master in Eng. M.R. Gutiérrez-Lara for her technical support.

References

[1] Water Environment Federation (WEF), Biofilm Reactors: Manual of Practice No. 35, McGraw-Hill, WEF Press, New York, 2010.
[2] C. Nicolella, M.C. van Loosdrecht, J.J. Heijnen, Wastewater treatment with particulate biofilm reactors, J. Biotechnol., 80 (2000) 1–33.

[3] M. González-Brambila, F. López-Isunza, Comportamiento de un reactor de biopelícula para tratamiento de agua residual a diferentes velocidades de flujo (Membrane-attached biofilm reactor behavior under different flow rate conditions in the treatment of a synthetic wastewater), Rev. Mex. Ing. Chim., 3 (2008) 183–193.
[4] D.G. Najafpour, Biochemical engineering and biotechnology, 1st Ed., Elsevier, Amsterdam, 2007.
[5] B. Arrojo, M. Figueroa, A. Mosquera-Corral, J.L. Campos, R. Méndez, Influence of gas flow-induced shear stress on the operation of the Anammox process in a SBR, Chemosphere, 72 (2008) 1687–1693.
[6] S. Chakraborty, E. Drioli, L. Giorno, Development of a two separate phase submerged biocatalytic membrane reactor for the production of fatty acids and glycerol from residual vegetable oil streams, Biomass Bioenergy, 46 (2012) 574–583.
[7] B. Jajuee, A. Margaritis, B. Karamanev, M.A. Bergoug, Kinetics of biodegradation of p-xylene and naphthalene and oxygen transfer in a novel airlift immobilized bioreactor, Biotechnol. Bioeng., 96 (2007) 232–243.
[8] I. Hutten, Handbook of Nonwoven Filter Media, 1st Ed., Elsevier, Oxford, 2007.
[9] Y.H. Lin, Modeling the performance of biodegradation of textile wastewater using polyurethane foam sponge cube as a supporting medium, Water Sci. Technol., 62 (2010) 2801–2810.
[10] Y.H. Lin, T.Y. Hsien, Kinematics of biodegradation of phenolic wastewater in a biofilm reactor, Water Sci. Technol., 59 (2009) 1703–1711.
[11] P.M. Kilonzo, A. Margaritis, M.A. Bergougnou, Hydrodynamics and mass transfer characteristics in an inverse internal loop airlift-driven fibrous-bed bioreactor, Chem. Eng. J., 157 (2010) 146–160.
[12] S.J. Russell, Handbook of Nonwovens, 1st Ed., Woodhead Publishing Limited, The Textile Institute, CRC Press, England, 2007.
[13] G. Besagni, P. Brazzale, A. Fiocca, F. Inzoli, Estimation of bubble size distributions and shapes in two-phase bubble column using image analysis and optical probes, Flow Meas. Instrum., 52 (2016) 190–207.
[14] D. Mamma, E. Kalogeris, N. Papadopoulos, D.G. Hatzinikolaou, P. Christrakopoulos, D. Kekos, Biodegradation of phenol by acclimatized *Pseudomonas putida* cells using glucose as an added growth substrate, J. Environ. Sci. Health, A39 (2004) 2093–2104.
[15] M.H. El-Naas, S.A. Al-Muhtaseb, S. Makhlouf, Biodegradation of phenol by *Pseudomonas putida* immobilized in polyvinylalcohol (PVA) gel, J. Hazard. Mater., 164 (2009) 720–725.
[16] American Public Health Association, Water Works Association, Water Environmental Federation, Standard Methods for the Examination of Water and Wastewater, 20th Ed, American Public Health Association, Washington, D.C., 1999.
[17] M. Mkandawire, J. Förster, D. Fiedler, H. Böttcher, W. Pompe, Spectrophotometric verification of biodegradation of phenol in a flow dynamic biocers-based bioreactor system, Int. J. Environ. Anal. Chem., 89 (2009) 529–541.
[18] A. Moser, Bioprocess technology, kinetics and reactors, Springer-Verlag, New York, 1988.
[19] O. Levenspiel, Chemical Reaction Engineering, 3rd Ed., John Wiley & Sons Inc., New York, 2004.
[20] M. Pirdashti, R. Kompany, Effects of height to diameter ratio and aeration rate on liquid mixing and hydrodynamic properties in a bubble column, Iran. J. Chem. Eng., 6 (2009) 46–56.
[21] Y. Chisti, Pneumatically agitated bioreactor in industrial and environmental bioprocessing: hydrodynamics, hydraulics, and transport phenomena. Appl. Mech. Rev., 51 (1998) 33–112.
[22] R.S. Ramalho, Introduction to Wastewater Treatment Processes, 2nd Ed., Academic Press, New York, 2003.
[23] F. Garcia-Ochoa, E. Gomez, Bioreactor scale-up and oxygen transfer rate in microbial processes: an overview, Biotechnol. Adv., 27 (2009) 153–176.
[24] H. Eberl, E. Morgenroth, D. Noguera, C. Picioreanu, B. Rittmann, M. Van Loosdrecht, O. Wanner, (IWA Task Group on Biofilm), Modeling, Mathematical Modeling of Biofilms, Scientific and Technical Report No. 18, 1st Ed., IWA Publishing, Hove, 2006.
[25] Y. Chisti, Hydrodynamic damage to animal cells, Crit. Rev. Biotechnol., 21 (2001) 67–110.
[26] P. Reichert, Design techniques of a computer program for the identification of processes and the simulation of water quality in aquatic systems, Environ. Software, 10 (1995) 199–210.
[27] P. Reichert, AQUASIM 2.0 Tutorial, Swiss Federal Institute for Environmental Science and Technology (EAWAG), CH-8600 Dübendorf, Switzerland, 1998.
[28] P. Reichert, AQUASIM 2.0 User Manual, Swiss Federal Institute for Environmental Science and Technology (EAWAG), CH-8600 Dübendorf, Switzerland, 1998.
[29] M. Bajaj, C. Gallert, J. Winter, Phenol degradation kinetics of aerobic mixed culture, Biochem. Eng. J., 46 (2009) 205–209.
[30] N. Kantarci, F. Borak, K.O. Ulgen, Bubble column reactors, Process Biochem., 40 (2005) 2263–2283.
[31] A. Pérez, P. Torres, Evaluación del comportamiento hidrodinámico como herramienta para optimización de reactores anaerobios de crecimiento en medio fijo (Evaluation of hydrodynamic behavior as a tool to optimize anaerobic reactors of attached growth), Antioquia, 45 (2008) 27–40.
[32] A.J. Guwy, S.R. Martin, F.R. Hawkes, D.L., Catalase activity measurements in suspended aerobic biomass and soil samples, Enzyme Microb. Technol., 25 (1999) 669–676.
[33] T. Kablan, Y.Y. Clément, K.A. Françoise, O.K. Mathias, Determination and modelling of moisture sorption isotherms of chitosan and chitin, Acta Chim. Slov., 55 (2008) 677–682.